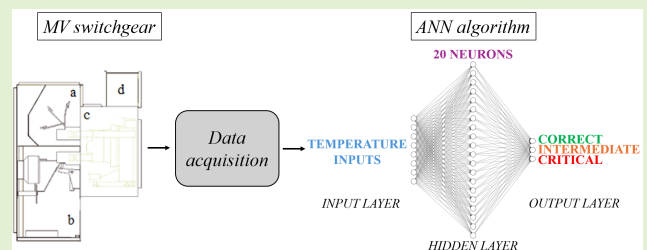


# Predictive Maintenance Based on Artificial Neural Network for MV Switchgears

Virginia Negri<sup>1</sup>, Graduate Student Member, IEEE, Grazia Iadarola<sup>2</sup>, Member, IEEE, Alessandro Mingotti<sup>1</sup>, Member, IEEE, Susanna Spinsante<sup>1</sup>, Senior Member, IEEE, Roberto Tinarelli<sup>1</sup>, Senior Member, IEEE, and Lorenzo Peretto<sup>1</sup>, Senior Member, IEEE

**Abstract**—The distribution network is recognized for its inherent fragility and challenging management compared to the transmission network. This challenge arises from the complex topology of the distribution network, involving thousands of nodes to monitor by predictive maintenance. This article introduces the implementation of an artificial neural network (ANN) for predictive maintenance of medium-voltage (MV) switchgears. In particular, the study here presented consists in proposing a new approach that correlates temperature measurements, at different positions within the switchgear, to potential faults. The specific cause of temperature change is the variable fastening in a single point of the MV switchgear. Thus, starting from experimental measurements, the ANN is thoroughly analyzed, compared, and validated to provide a proper classification of the switchgear health status. The obtained results affirm the efficacy of the proposed approach and highlight the benefits of its application in practical predictive maintenance scenarios.

**Index Terms**—Accuracy, artificial intelligence (AI), artificial neural network (ANN), distributed measurement systems, fault detection, machine learning (ML), medium-voltage (MV) switchgears, predictive maintenance, temperature monitoring, thermocouples.



## I. INTRODUCTION

MONITORING plays a crucial role in ensuring the robustness and reliability of both transmission and distribution networks within the electrical power systems. In transmission networks, which carry electricity over long distances, real-time monitoring is essential to track power flow, voltage levels,

and line capacities. Continuous surveillance of equipment, such as transformers and circuit breakers, is imperative to detect potential issues early and prevent catastrophic failures [1]. On the other hand, distribution networks, responsible for delivering electricity to end-users, demand monitoring at various nodes due to their intricate topology. Thousands of nodes in distribution networks necessitate comprehensive monitoring instrumentation to detect load imbalances, voltage fluctuations, and equipment malfunctions promptly. Both networks benefit from advanced monitoring technologies, including sensors and supervisory control and data acquisition (SCADA) systems [2]. This, to enhance situational awareness, optimize performance, and facilitate timely maintenance interventions, ensuring a resilient and efficient electricity supply to consumers.

Manuscript received 29 July 2024; revised 1 September 2024; accepted 3 September 2024. Date of publication 18 September 2024; date of current version 31 October 2024. This research has received funding from the project Vitality – Project Code ECS00000041, CUP I33C22001330007 - funded under the National Recovery and Resilience Plan (NRRP), Mission 4 Component 2 Investment 1.5 - Creation and strengthening of “innovation ecosystems”, construction of “territorial leaders in R&D” – Innovation Ecosystems - Project “Innovation, digitalization and sustainability for the diffused economy in Central Italy – VITALITY” Call for tender No. 3277 of 30/12/2021, and Concession Decree No. 0001057.23-06-2022 of Italian Ministry of University funded by the European Union – NextGenerationEU. The associate editor coordinating the review of this article and approving it for publication was Prof. Yongqiang Zhao. (Corresponding author: Grazia Iadarola.)

Virginia Negri, Alessandro Mingotti, Roberto Tinarelli, and Lorenzo Peretto are with the Department of Electric, Electronic and Information Engineering “G. Marconi,” University of Bologna, 40136 Bologna, Italy (e-mail: virginia.negri2@unibo.it; alessandro.mingotti2@unibo.it; roberto.tinarelli3@unibo.it; lorenzo.peretto@unibo.it).

Grazia Iadarola and Susanna Spinsante are with the Department of Information Engineering, Università Politecnica delle Marche, 60131 Ancona, Italy (e-mail: g.iadarola@staff.univpm.it; s.spinsante@staff.univpm.it).

Digital Object Identifier 10.1109/JSEN.2024.3455755

In smart grids, the choice between time-based maintenance and predictive maintenance approaches is pivotal for optimizing operational efficiency and ensuring system reliability [3]. Traditionally, time-based maintenance relies on predefined schedules for equipment checks and replacements, offering simplicity in execution but often leading to unnecessary interventions and resource inefficiencies [4]. On the contrary, predictive maintenance leverages advanced technologies such as distributed measurement systems [5] and artificial intelligence (AI) to anticipate potential failures based on real-time data and performance indicators. This proactive approach allows for targeted interventions, reducing downtime and

optimizing the lifespan of grid components. In the dynamic and interconnected landscape of smart grids, where real-time data are abundant, predictive maintenance emerges as a strategic choice, offering a more precise and cost-effective way to manage the complexities of modern distribution networks.

The article focuses on predictive maintenance to prevent faults in medium-voltage (MV) switchgears. As highlighted in [6], several quantities could be evaluated inside a MV switchgear. Thermal, mechanical, and partial discharge (PD) measurements can help early identification of abnormal conditions by means of AI [6]. The objective of this study is exactly to combine distributed measurement systems and machine learning (ML) to enhance predictive maintenance in MV switchgears. Specifically, the article proposes a new approach that leverages the correlation between potential fault and temperature measurements. Then, the temperature measurements are collected at different positions within a MV switchgear, and due to variable fastening in a single point of such MV switchgear. Indeed, the temperature variations, if properly correlated with fastening, can offer valuable information about the health status of the MV switchgear. The aforementioned correlation is then employed to implement an artificial neural network (ANN) fed with in-field temperature measurements. The innovation of the proposed method lies exactly in formulating an ANN for MV switchgears. It should be also noted that the proposed approach can be, more generally, applied to other input quantities different from temperature values considered in this study.

The remainder of the article is structured as follows. Section II presents an overview on the state-of-the-art of predictive maintenance in MV switchgears and ML-based methods, including the selected ANN algorithm. Section III serves as the core of the work, covering the case study description, with the involved equipment and the details on the ANN training and testing. Section IV presents the obtained results. In more detail, the algorithm and the proposed approach are first validated by simulations. Afterward, actual measurements, collected inside an operating MV switchgear, are used to prove the efficacy of the approach in practical applications. Final remarks are provided in Section V.

## II. PREDICTIVE MAINTENANCE AND ML

### A. Predictive Maintenance of MV Switchgears

This section seeks to offer an overview of current research pertaining to MV switchgears. Notably, a significant portion of the research investigates temperature rises resulting from normal/abnormal operations. For instance, the objective of [7] is to quantify temperature increases due to power losses. In [8], a thermal model is constructed to analyze the temperature rise at the connection points of the copper busbars. Similarly, the work presented in [9] delves into the creation of a thermal model capable of estimating temperature distributions within the switchgear.

In terms of the technology employed for measuring parameters such as temperature, current, and voltage, acoustic sensors are featured in [10] and [11]. The wireless nature of these sensors eliminates the need for physical attachment to the surface to measure. Study [12] contributes an insightful review of wireless temperature measurement techniques. Shifting toward more experimental endeavors, distributed measurement systems can be designed to detect PDs in MV switchgears [13], [14], [15]. Alternative options for predictive maintenance

in MV switchgears can be arc detection [16], [17], or sulfur hexafluoride monitoring [18]. Crucially, a distributed measurement system must be cost-effective, easy to install, and sufficiently accurate to warrant consideration for widespread deployment in electric cabinets.

AI is adopted in [19], where an algorithm is developed to estimate the temperature of the switchgear components. This algorithm leverages an a priori thermal model of the switchgear, showcasing the integration of AI in temperature estimation processes. Finally, the authors started this research with an experimental campaign described in [20].

### B. Current Status of ML-Based Predictive Maintenance

AI stands as a subfield within computer science, dedicated to replicating human intelligence processes through the implementation of computer programs. AI systems operate by processing extensive datasets, empowering effective problem-solving capabilities. One of the main reasons of AI significance in electrical engineering comes from the abundance of available data and information, provided for example by distributed measurement systems. In the spectrum of AI for predictive maintenance, several techniques of ML and deep learning emerge as salient [21]. ML enables algorithms to autonomously learn and improve by adapting to provided data using computational and mathematical techniques. In predictive maintenance for electrical facilities engineering, ML enhances power systems with self-adaptability and self-awareness, boosting network autonomy [22].

ML-based predictive maintenance applications can be divided into supervised and unsupervised learning approaches. In supervised learning, datasets include information about the system status, e.g., health status, remaining useful life (RUL) values, or fault types. Conversely, unsupervised learning algorithms lack maintenance-related data [23]. Focusing on supervised learning tasks, classification and regression problems are identified. The former arises for example when distinguishing between health and malfunction states [24], [25]. The latter comes into play when forecasting RUL [26] or another target variable. For instance, in [27], the objective is to implement AI-based thermal prognostic models predicting the likely temperature along a cable joint.

In the domain of energy systems, the primary focus in predictive maintenance research is directed toward high-power wind turbines [28]. In [29], a data-driven framework is introduced to predict faults in wind generators, comparing support vector machine (SVM), adaptive boosting algorithm, and ANN. Additionally, in [30], an ANN is applied to SCADA data to predict operating anomalies in the main components of wind turbines. Finally, in [31], various algorithms, including random forest (RF), ANN, SVM, and decision tree (DT), are evaluated for predicting the insulation health condition of MV distribution transformers based on their oil test results.

### C. Selected Algorithm

ANNs have gained widespread application in predictive maintenance tasks. However, within the realm of MV switchgears, the utilization of ANNs remains relatively uncommon. This study aims to address this gap by proposing an ANN for predictive maintenance of MV switchgears based on temperature measurements. Particularly, the proposed ANN is designed to establish a correlation between temperature

measurements within the switchgear and its health status. The case study is formulated as a multiclass classification task.

The fundamental architecture of an ANN comprises input, hidden, and output layers, with layers being vertical structures composed of elementary units known as neurons [32]. Each neuron is characterized by its activation function, dictating the input–output relation, and a bias value that introduces a shift to the input. The connections among neurons are defined by weights, indicating the strength of the interneuron connections.

Two distinct types of ANN models, feed-forward and recurrent neural networks, are recognized based on the direction of information flow. The former exhibits unidirectional information flow (from input to output layer), while the latter allows for bidirectional information flow, including backward propagation. The specific architecture of the ANN proposed in this study is a feed-forward neural network comprising three layers: input, hidden, and output layers. Furthermore, the chosen activation functions for hidden layer and output layer are, respectively, the rectified linear unit (ReLU), with 20 hidden neurons, and the Softmax. The choice of ReLU and Softmax is driven by several considerations. ReLU is a common choice for the activation function in hidden layers of ANNs because it is computationally efficient since it allows for faster convergence of the model, accelerating the training process [33]. In fact, ReLU activates only when the input is positive, providing greater learning capacity compared to other functions. Softmax is, instead, commonly used in the last layer of a neural network for multiclass classification problems. Indeed, it converts the network outputs into a probability distribution with sum equal to 1, making them interpretable as predicted probabilities for each class. In particular, for an  $N$ -size input vector  $\mathbf{x}$ , the following equations are implemented:

$$\text{ReLU} = \begin{cases} 0, & \text{if } x_i < 0 \\ x_i, & \text{if } x_i \geq 0 \end{cases} \quad (1)$$

$$\text{Softmax} = \frac{e^{x_i}}{\sum_{j=1}^N e^{x_j}}, \quad i = 1, 2, \dots, N \quad (2)$$

where  $x_i$  represents the  $i$ th element of  $\mathbf{x}$ . Finally, for training the network, the adaptive moment estimation optimizer is employed. Moreover, the implementation of the ANN is carried out using the Keras module of the TensorFlow library in the Python programming language.

### III. TEMPERATURE-BASED PREDICTIVE MAINTENANCE OF MV SWITCHGEAR

This section presents the case study for the temperature-based predictive maintenance of MV switchgears. The analysis method is described in Fig. 1. In summary, temperature values were acquired during an in-field measurement campaign. Subsequently, synthetic datasets are generated from these measurements to facilitate the training phase of the selected algorithm described in Section II-C. Finally, the efficacy of the algorithm is validated by using both simulated temperature values and actual temperature measurements.

#### A. Experimental Setup

The predictive maintenance herein proposed builds upon temperature measurements to carry out inside MV switchgears, which should comply with the International Standard IEC 62271-200. The experimental setup employed for the case study is composed by a MV switchgear and a data acquisition system to measure the temperature values.

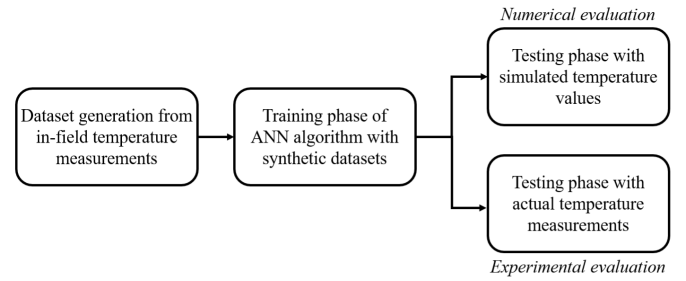


Fig. 1. Flowchart of the analysis method.

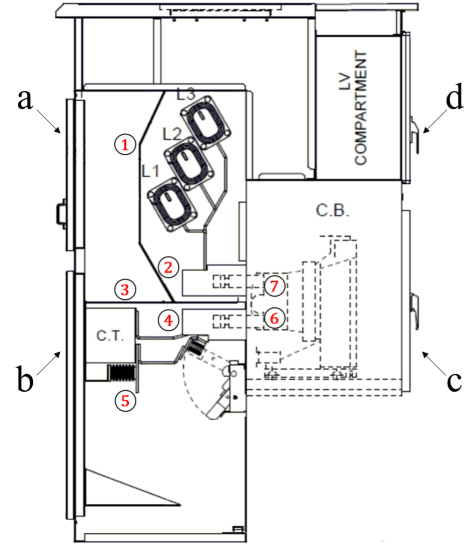


Fig. 2. Compartments of the MV switchgear and location of thermocouples.

The MV switchgear is an Imesa MINIVER/C MV switchgear, namely, a metal-closed switchboard, designed in compliance with the International Standard IEC 62271-200, for voltages above 1 kV and up to and including 52 kV. It consists of four main sections, shown in Fig. 2: a busbar compartment (a), a line compartment (b), a circuit breaker compartment (c), and a low-voltage compartment (d). The busbar compartment contains two copper busbars, linked by a joint, and connected to the fixed contact of a higher interrupting device envelope. The busbar compartment is supplied by a three-phase system, which branches off along all the MV compartments. Then, in the line compartment, the current is reduced by a factor of 750 through a WATTSUD IWR10K current transformer working at a frequency of 50 Hz. The line compartment is also designated for hosting the lines that connect the power cables, arranged in the rear part, to the fixed contact of a lower interrupting device envelope. Finally, the switchgear is endowed with an interrupting device and a low-voltage equipment, placed, respectively, in the circuit breaker compartment (c) and in the low-voltage compartment (d). The switchgear is supplied by a current of 630 A, generated at a frequency of 50 Hz.

In the correct operating conditions of the MV switchgear, the joint between the busbars as well as the connection to the power cables are fastened by torque wrench and M10 bolts with a torque of 45 Nm [20]. The fixed contacts with the two interrupting device envelopes, i.e., the former in the busbar compartment and the latter in the line compartment, as well

TABLE I  
MINIMUM AND MAXIMUM TEMPERATURE VALUES ACQUIRED DURING THE THREE SESSIONS BY FASTENING THE CURRENT TRANSFORMER WITH A TORQUE OF 60, 20, AND 4 Nm

thermocouple	temperature [°C] with 60 N m		temperature [°C] with 20 N m		temperature [°C] with 4 N m	
	minimum	maximum	minimum	maximum	minimum	maximum
1	42.1	44.2	43.2	45.3	42.7	45.1
2	51.1	53.5	52.3	54.6	52.7	55.2
3	52.0	55.0	66.8	69.3	81.9	86.9
4	53.7	56.2	59.0	61.3	63.3	66.4
5	43.9	46.4	54.4	56.8	62.4	65.2
6	53.4	55.8	57.5	59.8	60.8	63.7
7	51.3	53.7	52.9	55.3	52.9	55.5

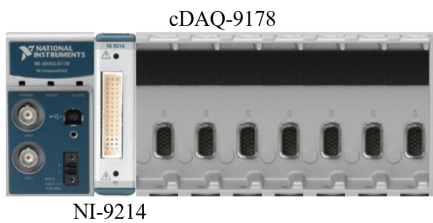


Fig. 3. Data acquisition system with cDAQ-9178 CompactDAQ chassis, equipped with single NI-9214 Temperature Input Module.

as the lower and upper tulips of the circuit breaker are, instead, fastened by M16 bolts with torque of 165 Nm [20]. At last, the current transformer is fastened by M12 bolts with a torque of 60 Nm [20].

Three separate sessions for temperature acquisition were carried out. In the first session, the correct operating conditions of the MV switchgear were observed, as described above. In the successive sessions, the fastening on the current transformer was progressively loosened, keeping all the other fastenings at the correct operating conditions. In detail, for the second acquisition, the current transformer was fastened with a torque of 20 Nm, while, for the third acquisition, the current transformer was fastened with a torque of 4 Nm.

The temperature values were measured by a set of seven TC SR30KX K-type thermocouples, located inside the switchgear. The thermocouples were distributed to measure differential temperature in seven points of the MV switchgear and circled in Fig. 2: 1) joint between the busbars; 2) fixed contact with the higher interrupting device envelope in the busbar compartment; 3) top contact with the current transformer; 4) fixed contact with the lower interrupting device envelope in the line compartment; 5) connection to the power cables; 6) lower tulip; and 7) upper tulip of the circuit breaker.

The thermocouples were connected to a data acquisition system consisting of a National Instruments cDAQ-9178 CompactDAQ chassis, equipped with a National Instruments NI-9214 C Series Temperature Input Module [34] and represented in Fig. 3. The NI-9214 Temperature Input Module of the cDAQ-9178 CompactDAQ chassis converts the temperature-dependent voltage from the thermocouples in temperature values. The NI-9214 Temperature Input Module can acquire up to 16 thermocouple input channels. Thus, a single module is enough to measure simultaneously the temperature values from seven thermocouples, occupying only one of the eight slots of the cDAQ-9178 CompactDAQ chassis, as shown in Fig. 3.

In order to observe the different temperature increase due to the three fastenings, each acquisition session started only 5 h and 35 min after turning on the switchgear.

Then, 50 temperature values were acquired by each thermocouple, one every 2 min and 30 s since the beginning of the session. The minimum and maximum values of the temperature acquired during the three sessions, by fastening the current transformer with a torque of 60, 20, and 4 Nm, are reported in Table I.

According to the IEC 62271-200, MV switchgears work in normal operating conditions if their external air temperature falls in the range  $[-5.0^{\circ}\text{C}, 40.0^{\circ}\text{C}]$ . For this reason, two K-type thermocouples were located outside the switchgear for the three sessions, measuring air temperature values on average equal to  $18.9^{\circ}\text{C}$ ,  $19.1^{\circ}\text{C}$ , and  $18.2^{\circ}\text{C}$ , respectively. Thus, the external air temperature values during the experimental tests are within the range limits. As a rule, the environmental conditions of MV switchgears should be controlled in order to guarantee that the external air temperature is within the specified range. Obviously, should the environmental conditions bring to uncontrolled variations outside the limits set by the IEC 62271-200, the switchgear operation would not be bound to the temperature values expected by predictive maintenance.

## B. Dataset Generation

In order to implement the ANN, training and testing stages are required. To this aim, synthetic datasets representative of the three fastenings are created from the in-field temperature measurements. The specific decision of creating synthetic datasets is rooted to the fact that ANN models typically need extensive training to achieve optimal performance, a requirement often unmet by solely in-field measurements.

For dataset generation, 1000 temperature values are synthetically generated from a uniform distribution for each thermocouple and each fastening. In particular, the uniform distribution is centered on the mean value of the 50 temperature values acquired by each thermocouple for each fastening, as described in Section III-A. Instead, as concerns the interval limits of the uniform distribution, the choice is guided by typical measurement uncertainty associated with sensors employed in this application scenario, according to the International Standard IEC 60751. Therefore, for a numerical evaluation, described in Section IV-B, two extreme cases are considered, i.e., with uncertainty equal to  $\pm 0.5^{\circ}\text{C}$  and  $\pm 1.5^{\circ}\text{C}$ . Subsequently, for an experimental evaluation, described in Section IV-C, the uncertainty is set to  $\pm 1.0^{\circ}\text{C}$ , as provided by the specifications of the adopted data acquisition system [34]. Definitely, the datasets for each fastening consist of 7000 temperature values, for a total dataset of 21 000 temperature values.

## C. Algorithm Implementation

The ANN model described in Section II-C is characterized by simplicity and high performance. Fig. 4 depicts the block

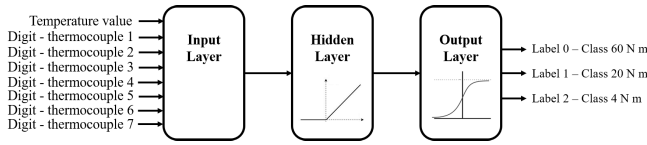


Fig. 4. Block scheme of the ANN with its activation functions.

scheme of the considered network, pointing out input features and output labels, as well as the activation functions of hidden and output layers.

The input features of the model comprise the temperature value and the corresponding number of the measuring thermocouple, for eight input features altogether. Clearly, the thermocouple number is indicative of the measurement point inside the MV switchgear. In order to enhance performance, particular attention is given to data preprocessing, ensuring that the model can effectively leverage the input features to achieve optimal results. Specifically, the temperature values are normalized between 0 and 1. Instead, the thermocouple number, ranging from 1 to 7, is encoded by one-hot encoding. The one-hot encoding technique is commonly used to convert categorical data into binary vectors. In this case study, characterized by the seven thermocouples, the first vector is represented as [1, 0, 0, 0, 0, 0, 0], while the last vector is represented as [0, 0, 0, 0, 0, 0, 1]. Thus, the seven vectors, one for each thermocouple, are the actual input features of the ANN model, along with the temperature value. As concerns the output, three distinct classes are identified for each torque value: 60, 20, and 4 Nm labeled, respectively, as 0, 1, and 2, and corresponding to correct, intermediate, and critical operating conditions.

#### IV. RESULTS

This section consists of three parts. Initially, the definition of the metrics used for the evaluation of the tests is given. Then, the results of the preliminary testing performed with the synthetic data are given. Finally, the results of algorithm testing, using experimental data, are discussed.

##### A. Evaluation Metrics

Concerning the evaluation of the ANN model performance, various metrics are available to assess its classification outcomes. The definition of metrics involves the identification of true positive (TP), true negative (TN), false positive (FP), and false negative (FN) cases. TP and TN represent correctly predicted values, while FP and FN denote noncorrectly predicted values. In the context of a binary classification task, TP and TN count instances where positive (1) and negative (0) values are predicted as 1 and 0 by the model, respectively. Conversely, FP and FN represent cases where 0 and 1 values are predicted as 1 and 0. Confusion matrix is an effective visual representation of classifier results. Principal diagonal cases represent the correct predictions made by the algorithm, while other cells contain the mistaken values.

Accuracy assesses the overall correctness of the model

$$\text{Accuracy} = \frac{\text{TP} + \text{TN}}{\text{TP} + \text{FP} + \text{TN} + \text{FN}} \times 100\%. \quad (3)$$

Therefore, in what follows, the Accuracy is presented as a unique value that assesses the model performance and not as a parameter evaluated for each of the  $K$  considered classes.

Precision quantifies the ratio of correctly predicted positive values to the predicted positive values

$$\text{Precision}(k) = \frac{\text{TP}(k)}{\text{TP}(k) + \text{FP}(k)} \times 100\%, \quad k = 1, 2, \dots, K. \quad (4)$$

High Precision relates to the low false-positive rate.

Sensitivity expresses the ratio of correctly predicted positive values to the actual positive values

$$\text{Sensitivity}(k) = \frac{\text{TP}(k)}{\text{TP}(k) + \text{FN}(k)} \times 100\%, \quad k = 1, 2, \dots, K. \quad (5)$$

For a comprehensive evaluation of model performance, both Precision and Sensitivity should be considered. Thus, the  $F_1$  score serves as a helpful metric that incorporates both Precision and Sensitivity

$$F_1(k) = 2 \frac{(4) \times (5)}{(4) + (5)} \times 100\%, \quad k = 1, 2, \dots, K. \quad (6)$$

Since the proposed case study is formulated as a multiclass classification task, a note on metrics calculation is required. Precision, Sensitivity, and  $F_1$  can be computed for each class individually or averaged across all classes. The averaging approach includes macroaveraging, which calculates scores for each class individually and then averages them. The macroaverage of Precision, Sensitivity, and  $F_1$  are, respectively, calculated as

$$\text{macro-average}_{\text{Precision}} = \frac{1}{K} \sum_{k=1}^K \text{Precision}(k) \quad (7)$$

$$\text{macro-average}_{\text{Sensitivity}} = \frac{1}{K} \sum_{k=1}^K \text{Sensitivity}(k) \quad (8)$$

$$\text{macro-average}_{F_1} = \frac{1}{K} \sum_{k=1}^K F_1(k). \quad (9)$$

In reality, other methods of averaging metrics include microaverage and weighted average. However, the microaverage, when calculated for each metric, always matches the Accuracy value. This happens because, in multiclass classification, the microaverage aggregates the contributions of all classes by summing their TP, FN, and FP, which is exactly the computation of Accuracy. Similarly, the weighted average is equivalent to the macroaverage because each class has the same number of instances, making the weights equal across all classes.

##### B. Numerical Evaluation

The two datasets consisting of 21 000 synthetic temperature values with uncertainty, respectively,  $\pm 0.5^\circ\text{C}$  and  $\pm 1.5^\circ\text{C}$ , described in Section III-B, are employed for the numerical evaluation. Then, for both the datasets, the 80% is considered for training, while the remaining 20% is reserved for testing.

Table II reports, for each dataset, the Accuracy values and the execution times of training and testing phases. The results derived from testing the ANN model on the datasets with uncertainty  $\pm 0.5^\circ\text{C}$  and  $\pm 1.5^\circ\text{C}$  are compiled in Tables III and IV, respectively. In these tables, the first three rows present the Precision, Sensitivity, and  $F_1$  metrics for the three output classes. Focusing on the results obtained

**TABLE II**  
OVERALL PERFORMANCE AND EXECUTION TIMES  
FOR SYNTHETIC DATASETS

Uncertainty value	Accuracy (%)	Training time [s]	Testing time [s]
$\pm 0.5^\circ\text{C}$	83.38	21.92	0.35
$\pm 1.5^\circ\text{C}$	77.48	20.66	0.33

**TABLE III**  
METRICS FOR SYNTHETIC DATASET WITH UNCERTAINTY  $\pm 0.5^\circ\text{C}$

	Precision (%)	Sensitivity (%)	$F_1$ (%)
60 N m Class	100.00	91.79	95.72
20 N m Class	66.73	100.00	80.05
4 N m Class	100.00	58.36	73.70
macro-averages	88.91	83.38	83.16

**TABLE IV**  
METRICS FOR SYNTHETIC DATASET WITH UNCERTAINTY  $\pm 1.5^\circ\text{C}$

	Precision (%)	Sensitivity (%)	$F_1$ (%)
60 N m Class	86.89	81.93	84.34
20 N m Class	67.72	76.57	71.87
4 N m Class	79.80	73.93	76.75
macro-averages	78.14	77.48	77.65

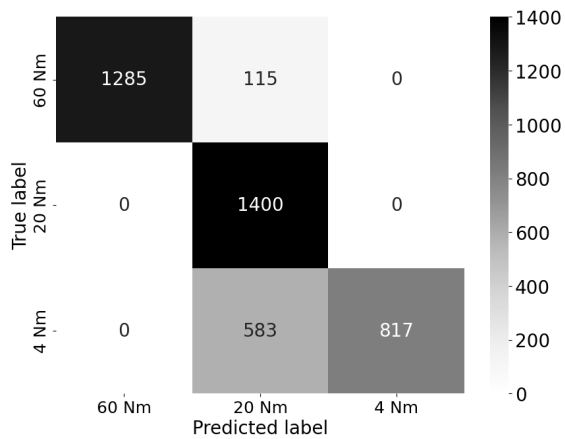


Fig. 5. Confusion matrix for synthetic dataset with uncertainty  $\pm 0.5^\circ\text{C}$ .

for the dataset with uncertainty  $\pm 0.5^\circ\text{C}$ , different outcomes emerge depending on the specific class under consideration. The 60Nm class exhibits the highest values among all the three metrics, while the 4Nm class yields the least favorable results. On a global scale, the average values for all the metrics exceed the 83%. Increasing measurement uncertainty leads to a performance decrease. Regarding the results for the dataset with uncertainty  $\pm 1.5^\circ\text{C}$ , the average values exceed the 77%. The poorest metric values are observed when classifying instances of the 20Nm class.

For a comprehensive evaluation of the classifier results, Figs. 5 and 6 show, respectively, the confusion matrices obtained for the synthetic datasets with uncertainty  $\pm 0.5^\circ\text{C}$  and  $\pm 1.5^\circ\text{C}$ . Predominantly, instances belong to the principal diagonal, indicating accurate classification performance. Notably, in the case of uncertainty  $\pm 0.5^\circ\text{C}$ , no instances of the 60Nm class are misclassified as 4Nm values, and vice-versa. This observation underscores the model ability to consistently predict both the best and worst fastenings, demonstrating that only neighboring classes may undergo classification interchange. As the uncertainty increases, the classification

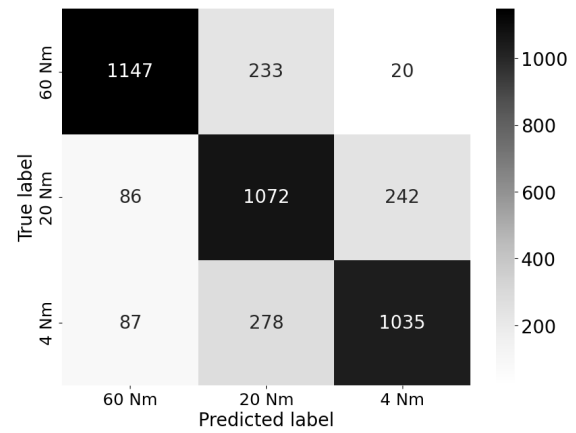


Fig. 6. Confusion matrix for synthetic dataset with uncertainty  $\pm 1.5^\circ\text{C}$ .

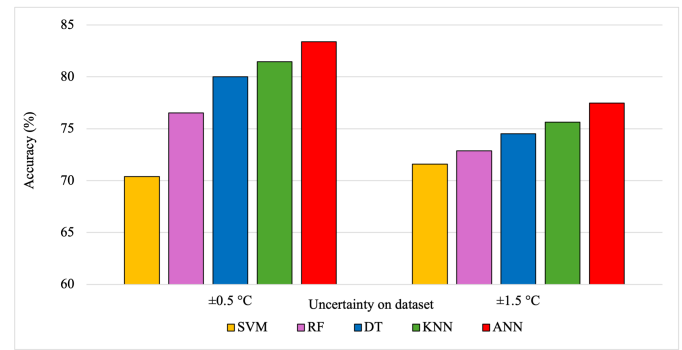


Fig. 7. Comparison of algorithms in terms of Accuracy.

performance diminishes. This result is predictable due to the nature of the adopted algorithm.

In addition, for the sake of completeness, the selected algorithm is compared to several ML algorithms. Specifically, the following algorithms are implemented and assessed for temperature-based predictive maintenance of the MV switchgear: SVM, RF, DT, and  $k$ -nearest neighbors ( $K$ -NN). SVM is widely used in predictive maintenance tasks due to its effectiveness in high-dimensional spaces. RF and DT are renowned for their high performance and interpretability in classification tasks.  $K$ -NN is favored for its simplicity and adaptability. In this scenario, all the models are trained with the 80% of datasets with uncertainty  $\pm 0.5^\circ\text{C}$  and  $\pm 1.5^\circ\text{C}$  and tested with the remaining 20%. The comparison results illustrated in Fig. 7 demonstrate that the proposed ANN model achieves higher performance for both the uncertainty values.

### C. Experimental Evaluation

The experimental evaluation is intended to assess the effectiveness of the ANN in practical settings. In this case, the synthetic dataset with uncertainty  $\pm 1.0^\circ\text{C}$  is employed for the training phase. Then, the testing phase is implemented on the actual temperature measurements obtained as described in Section III-A. Therefore, the testing datasets for each fastening consist of 350 measurement values, corresponding to 1050 temperature measurements on the whole.

Table V shows the reached value of Accuracy for the experimental measurements and the execution times for both the phases of training and testing. Table VI presents the other metrics. The metric values exceed the 78%,

TABLE V  
OVERALL PERFORMANCE AND EXECUTION TIMES  
FOR EXPERIMENTAL MEASUREMENTS

Uncertainty value	Accuracy (%)	Training time [s]	Testing time [s]
$\pm 1.0^{\circ}\text{C}$	78.38	22.18	0.28

TABLE VI  
METRICS FOR EXPERIMENTAL MEASUREMENTS

	Precision (%)	Sensitivity (%)	$F_1$ (%)
60 N m Class	87.54	84.29	85.88
20 N m Class	68.93	75.43	72.03
4 N m Class	80.00	75.43	77.65
macro-averages	78.82	78.38	78.52

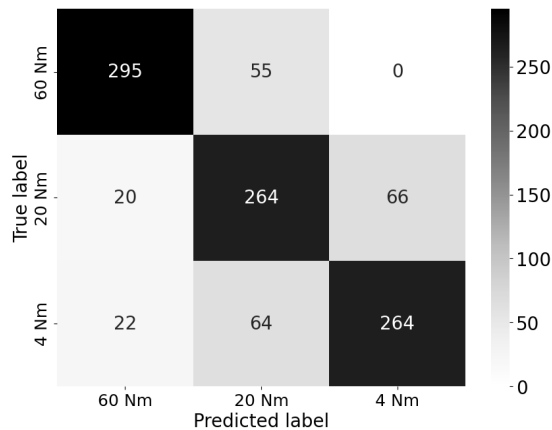


Fig. 8. Confusion matrix for experimental measurements.

which is a good outcome. Additionally, Fig. 8 displays the corresponding confusion matrix.

## V. CONCLUSION

The goal of this article is to enhance fault location strategies for improved predictive maintenance in MV switchgears. It proposes the integration of ANN with a distributed measurement system that collects temperature data. These temperature values, collected from within the switchgear, are correlated with the switchgear health status using AI. A key novelty of this article is linking temperature changes, resulting from varying component fastening levels within the switchgear, to the asset condition. This advanced health status monitoring allows for the immediate detection of malfunctions, enabling system operators to implement predictive maintenance strategies effectively.

The article provides a detailed description of the network and experimental setup, followed by an account of algorithm training and testing. The ANN has been evaluated both on synthetic data and actual data from a measurement campaign. The high level of Accuracy obtained on the numerical and experimental data proves that the proposed method is suitable for health assessment of MV switchgears. Generally speaking, the results strongly support the benefits of implementing a predictive maintenance approach that combines distributed measurements and ML algorithms.

## ACKNOWLEDGMENT

The contribution of IMESA SpA, Jesi (Ancona), Italy, is also acknowledged, for providing the MV switchgear required to perform the experimental campaign.

## REFERENCES

- [1] L. Zhang, J. Ruan, Z. Du, D. Huang, and Y. Deng, "Transmission line tower failure warning based on FBG strain monitoring and prediction model," *Electr. Power Syst. Res.*, vol. 214, Jan. 2023, Art. no. 108827.
- [2] R. Dutta, S. Chakrabarti, and A. Sharma, "Topology tracking for active distribution networks," *IEEE Trans. Power Syst.*, vol. 36, no. 4, pp. 2855–2865, Jul. 2021.
- [3] H. M. Hashemian, "State-of-the-art predictive maintenance techniques," *IEEE Trans. Instrum. Meas.*, vol. 60, no. 1, pp. 226–236, Jan. 2011.
- [4] Y. Merizalde, L. Hernández-Callejo, O. Duque-Perez, and V. Alonso-Gómez, "Maintenance models applied to wind Turbines. A comprehensive overview," *Energies*, vol. 12, no. 2, p. 225, Jan. 2019.
- [5] A. Mingotti et al., "Low-cost monitoring unit for MV cable joints diagnostics," in *Proc. IEEE 9th Int. Workshop Appl. Meas. Power Syst. (AMPS)*, Sep. 2018, pp. 1–5.
- [6] M. W. Hoffmann et al., "Integration of novel sensors and machine learning for predictive maintenance in medium voltage switchgear to enable the energy and mobility revolutions," *Sensors*, vol. 20, no. 7, p. 2099, Apr. 2020.
- [7] A. E. Seker, E. Aslan Sakaci, A. Deniz, B. Celik, and D. Yildirim, "Thermal analyses for a simplified medium-voltage switchgear: Numerical and experimental benchmark studies," in *Proc. 11th Int. Conf. Electr. Electron. Eng. (ELECO)*, Nov. 2019, pp. 116–120.
- [8] S. W. Park and H. Cho, "A practical study on electrical contact resistance and temperature rise at the connections of the copper busbars in switchgears," in *Proc. IEEE 60th Holm Conf. Electr. Contacts (Holm)*, Oct. 2014, pp. 1–7.
- [9] X. Wang et al., "Precise multi-dimensional temperature-rise characterisation of switchgear based on multi-conditional experiments and LPTN model for high-capacity application," *High Voltage*, vol. 6, no. 1, pp. 138–148, Feb. 2021.
- [10] G.-M. Ma et al., "A wireless and passive online temperature monitoring system for GIS based on surface-acoustic-wave sensor," *IEEE Trans. Power Del.*, vol. 31, no. 3, pp. 1270–1280, Jun. 2016.
- [11] X. Zhou and T. Schoepf, "Characteristics of overheated electrical joints due to loose connection," in *Proc. IEEE 57th Holm Conf. Electr. Contacts (Holm)*, Sep. 2011, pp. 1–7.
- [12] A. Dragomir, M. Adam, S.-M. Antohi, D. Murgoci, and A. Pantiru, "Temperature monitoring of MV switchgear cabinet by non-intrusive methods," in *Proc. 10th Int. Conf. Modern Power Syst. (MPS)*, Jun. 2023, pp. 1–4.
- [13] G. A. Hussain, A. A. Zaher, D. Hummes, M. Safdar, and M. Lehtonen, "Hybrid sensing of internal and surface partial discharges in air-insulated medium voltage switchgear," *Energies*, vol. 13, no. 7, p. 1738, Apr. 2020.
- [14] G. C. Montanari, R. Ghosh, L. Cirioni, G. Galvagno, and S. Mastroeni, "Partial discharge monitoring of medium voltage switchgears: Self-condition assessment using an embedded bushing sensor," *IEEE Trans. Power Del.*, vol. 37, no. 1, pp. 85–92, Feb. 2022.
- [15] Y. Otake and H. Murase, "Improving the estimation of partial discharge direction using a four-terminal surface current sensor," *Energies*, vol. 16, no. 21, p. 7389, Nov. 2023.
- [16] H. Kabashima and F. Kasahara, "Experimental study of high energy arcing faults using medium voltage metalclad switchgears," *Nucl. Technol.*, vol. 205, no. 5, pp. 694–707, May 2019.
- [17] F. Ore and M. Lehtonen, "Novel approach for the monitoring of single phase-to-ground fault associated with power arc," *Int. Rev. Electr. Eng.*, vol. 17, no. 6, pp. 544–555, 2022.
- [18] P. Billen, B. Maes, M. Larrain, and J. Braet, "Replacing SF<sub>6</sub> in electrical gas-insulated switchgear: Technological alternatives and potential life cycle greenhouse gas savings in an EU-28 perspective," *Energies*, vol. 13, no. 7, p. 1807, Apr. 2020.
- [19] J. Li, Y. Sun, N. Dong, and Z. Zhao, "A novel contact temperature calculation algorithm in distribution switchgears for condition assessment," *IEEE Trans. Compon., Packag., Manuf. Technol.*, vol. 9, no. 2, pp. 279–287, Feb. 2019.
- [20] S. Spinsante, G. Iadarola, G. Mazzocchi, and C. Romagnoli, "Temperature rise in MV switchgears: The role of loose busbar joints," in *Proc. 25th IMEKO TC-4 Int. Symp. Meas. Electr. Quantities, IMEKO TC-4 23rd Int. Workshop ADC DAC Modeling Test., (IWADC)*, 2022, pp. 51–56.
- [21] C. Chen, J. Shi, M. Shen, L. Feng, and G. Tao, "A predictive maintenance strategy using deep learning quantile regression and kernel density estimation for failure prediction," *IEEE Trans. Instrum. Meas.*, vol. 72, pp. 1–12, 2023.

- [22] S. Zhao, F. Blaabjerg, and H. Wang, "An overview of artificial intelligence applications for power electronics," *IEEE Trans. Power Electron.*, vol. 36, no. 4, pp. 4633–4658, Apr. 2021.
- [23] G. A. Susto, A. Schirru, S. Pampuri, S. McLoone, and A. Beghi, "Machine learning for predictive maintenance: A multiple classifier approach," *IEEE Trans. Ind. Informat.*, vol. 11, no. 3, pp. 812–820, Jun. 2015.
- [24] C. Chang, C. Lai, and R. Wu, "Decision tree rules for insulation condition assessment of pre-molded power cable joints with artificial defects," *IEEE Trans. Dielectr. Electr. Insul.*, vol. 26, no. 5, pp. 1636–1644, Oct. 2019.
- [25] I. Ullah et al., "Predictive maintenance of power substation equipment by infrared thermography using a machine-learning approach," *Energies*, vol. 10, no. 12, p. 1987, Dec. 2017.
- [26] A. Bracale, P. De Falco, L. P. D. Noia, and R. Rizzo, "Probabilistic state of health and remaining useful life prediction for Li-ion batteries," *IEEE Trans. Ind. Appl.*, vol. 59, no. 1, pp. 578–590, Jan. 2023.
- [27] P. L. Lewin, T. Coleman, N. Koumbari, Y. Liu, and S. Christou, "Avoiding medium voltage cable joint failure: Development of a real-time prognostic tool," in *Proc. IEEE Electr. Insul. Conf. (EIC)*, Jun. 2021, pp. 181–184.
- [28] S. Barja-Martinez, M. Aragüés-Peñalba, Ì. Munné-Collado, P. Lloret-Gallego, E. Bullich-Massagué, and R. Villafañila-Robles, "Artificial intelligence techniques for enabling big data services in distribution networks: A review," *Renew. Sustain. Energy Rev.*, vol. 150, Oct. 2021, Art. no. 111459.
- [29] E. Mammadov, M. Farrokhbadi, and C. A. Cañizares, "AI-enabled predictive maintenance of wind generators," in *Proc. IEEE PES Innov. Smart Grid Technol. Eur. (ISGT Europe)*, Oct. 2021, pp. 1–5.
- [30] A. Santolamazza, D. Dadi, and V. Introna, "A data-mining approach for wind turbine fault detection based on SCADA data analysis using artificial neural networks," *Energies*, vol. 14, no. 7, p. 1845, Mar. 2021.
- [31] A. Alqudsi and A. El-Hag, "Application of machine learning in transformer health index prediction," *Energies*, vol. 12, no. 14, p. 2694, Jul. 2019.
- [32] I. Goodfellow, Y. Bengio, and A. Courville, *Deep Learning*. Cambridge, MA, USA: MIT Press, 2016. [Online]. Available: <http://www.deeplearningbook.org>
- [33] D. C. Marcu and C. Grava, "The impact of activation functions on training and performance of a deep neural network," in *Proc. 16th Int. Conf. Eng. Modern Electr. Syst. (EMES)*, Jun. 2021, pp. 1–4.
- [34] *National Instruments: NI-9214 Specifications*. Accessed: Jul. 2024. [Online]. Available: <https://www.ni.com/docs/en-US/bundle/ni-9214-specs/page/specs.html>

**Virginia Negri** (Graduate Student Member, IEEE) was born in Bologna, Italy, in 1998. She received the B.S. degree in computer science engineering and the M.S. degree in electrical engineering from the University of Bologna, Bologna, in 2020 and 2022, respectively, where she is currently pursuing the Ph.D. degree in electrical engineering.

Her research interests include AI-based distributed measurement architectures in electrical power systems.

**Grazia Iadarola** (Member, IEEE) received the bachelor's (cum laude) degree in telecommunications engineering, the master's (cum laude) degree in electronic engineering, and the Ph.D. degree in information technologies for engineering from the University of Sannio, Benevento, Italy, in 2013, 2015, and 2019, respectively.

She is currently an Assistant Professor of Electrical and Electronic Measurements with the Polytechnic University of Marche, Ancona, Italy. Her research interests include sub-Nyquist sampling, characterization and testing of data converters, modeling of electronic circuits and nonidealities, and signal reconstruction based on compressed sensing, as well as their applications to telecommunications and biomedical instrumentation.

**Alessandro Mingotti** (Member, IEEE) was born in Cento, Italy, in 1992. He received the B.S., M.S. and Ph.D. degrees in electrical engineering from the University of Bologna, Bologna, Italy, in 2014, 2016, and 2020, respectively.

He is currently a Senior Assistant Professor with the University of Bologna. He is also working on several European Project H2020. His research interests include management and condition maintenance of distribution networks, development, modeling, and metrological characterization of instrument transformers.

Dr. Mingotti is an Associate Editor of IEEE TRANSACTIONS ON INSTRUMENTATION AND MEASUREMENT.

**Susanna Spinsante** (Senior Member, IEEE) received the Ph.D. degree in electronics and telecommunications engineering from Università Politecnica delle Marche, Ancona, Italy, in 2005.

She is currently an Associate Professor of Electrical and Electronic Measurements with the Department of Information Engineering (DII), Università Politecnica delle Marche. She co-authored more than 200 articles in international peer reviewed journals and conference proceedings. Her research interests are focused on the use of wearable sensors for the extraction of measurement signals applied to human monitoring, skin conductance acquisition and processing, and smart sensing systems for industrial applications.

Dr. Spinsante is a member of the IEEE Instrumentation and Measurement Society, the IEEE Signal Processing Society, GMEE, and CNIT. She is an Associate Editor of IEEE TRANSACTIONS ON INSTRUMENTATION AND MEASUREMENT.

**Roberto Tinarelli** (Senior Member, IEEE) received the M.S. degree in electrical engineering from the University of Bologna, Bologna, Italy, in 2000, and the Ph.D. degree in electrical engineering from the Polytechnic of Milan, Milan, Italy, in 2004.

He is currently a Full Professor of Electrical Measurements with the Department of "Guglielmo Marconi", University of Bologna. He has authored or co-authored more than 160 scientific papers, one book, and Co-Inventor of some WO patents in the field of sensors and instrument transformers. His research interests include devoted to design and metrological characterization of instruments for measurement under nonsinusoidal conditions; design and characterization of new electromagnetic-fields sensors and instrumentation; reliability study of electronic devices.

**Lorenzo Peretto** (Senior Member, IEEE) is a Professor of Electrical and Electronic Measurements with the University of Bologna, Bologna, Italy. He has authored or co-authored more than 200 papers, 24 patents, and three books. He is a Consultant of Industries Operating in the field of instrumentation and sensors for electrical measurements. His research interest include design and calibration of voltage and current instrument transformers (LPIT) for medium and high-voltage power networks; the design and realization of calibration systems of voltage and current instrument transformers; measurements of electrical quantities in power networks.

Dr. Peretto is a member of the IEEE Instrumentation and Measurement Society. He is the Chair of the annual IEEE Applied Measurements for Power System Conference, a member of the IEC TC38 "Instrument Transformers" and the Chair of the TC38/WG45 "Standard Mathematical Models for Instrument Transformers" and of the TC38/WG53 "Uncertainty evaluation in the calibration of Instrument Transformers."